Asian Journal of Chemistry; Vol. 36, No. 5 (2024), 1101-1108

ASIAN JOURNAL OF CHEMISTRY

https://doi.org/10.14233/ajchem.2024.31361

Antibacterial Activity of Silver Nanoparticles Synthesized from Endophytic *Streptomyces* sp. CR 13 Isolated from the Roots of *Ocimum tenuiflorum* L.

CHINNASAMY CHINNARAJU[1], CHINNAPERAMANOOR MADHU GANESAN[2], KANDASAMY PRABAKAR[2] and A.R. LAVANYA[1,*]

[1]P.G. & Research Department of Botany, Thanthai Periyar Government Arts and Science College (Autonomous) (Affiliated to Bharathidasan University), Tiruchirappalli-620023, India
[2]P.G. & Research Department of Zoology, Jamal Mohamed College (Autonomous) (Affiliated to Bharathidasan University), Tiruchirappalli-620020, India

*Corresponding author: E-mail: lavanyaar2021@gmail.com

Received: 6 February 2024; *Accepted*: 19 March 2024; *Published online*: 30 April 2024; AJC-21615

In this study, *Streptomyces* sp. CR 13 from the roots of *Ocimum tenuiflorum* L. was isolated and characterized using biochemical, morphological and genomic approaches. Silver nanoparticles (AgNPs) were synthesized extracellularly using cell-free extract and characterized with UV-vis spectroscopy, Fourier transform infrared (FTIR) spectroscopy, transmission electron microscopy (TEM), X-ray diffraction (XRD), EDX, DLS and zeta potential techniques. The maximum peak of UV-visible spectroscopy was observed at 425 nm and the TEM images revealed that the nanoparticles were spherical in shape and ranged in size from 18 to 21 nm. DLS analysis revealed particles with an average diameter of 147.9 nm. The zeta potential analysis of biosynthesized AgNPs showed a peak at -35.2 mV, indicating their high stability. Moreover, AgNPs synthesized by endophytic *Streptomyces* showed significant antimicrobial activity against *Escherichia coli*, *Klebsiella pneumonia* and *Stphylococcus aureus*.

Keywords: Endophyte, *Streptomyces*, *Ocimum tenuiflorum* L., Silver nanoparticles, Antibacterial activity.

INTRODUCTION

In nanotechnology, materials are developed at the nanoscale level (typically between 1 and 100 nm) to obtain unique properties and desired dimensions [1]. In most cases, nanomaterials are synthesized using chemical, physical and biological processes [2,3]. There have been many ways in which nanotechnology has been applied in the past few years, including imaging [4], biosensing [5], targeted medication administration [6], gene delivery systems [7] and artificial implants in the field of medical research [8]. Research on nanoparticles of polymers and metals is one of the most recent developments in nanotechnology. As a result, nanotechnology applications are becoming increasingly dependent on synthesizing nanoparticles with different shapes, sizes and chemical compositions. In addition, the catalytic, optical and electrical properties of metal nanoparticles have made them extremely important in recent years [9,10]. A variety of pharmacological effects of nanoparticles have been demonstrated, including antibacteriostatic [11], biofilm-eliminating [12], antifungal [13], anticancer [14] and antiviral [15] effects.

Thus, the development of nano-based drug is an active subject of research. As a result of the development of nanotechnology, microbial synthesis of AgNPs has been widely employed to alleviate toxic effects rather than relying on hazardous chemicals [16,17]. *Streptomyces* are filamentous, Gram-positive bacteria that possess a mycelial structure and are aerobic [18]. In natural drug discovery, they have been extensively investigated [19]. Recent years have witnessed a significant surge of interest in using *Streptomyces* to synthesize nanomaterials [20]. Despite this, there is little research on using endophytic *Streptomyces* to synthesize AgNPs. In plants, endophytic microorganisms have been shown to form a symbiotic relationship with their hosts' leaves, branches and roots without causing harmful effects [21-23]. Within the endophytic community, actinobacteria were most abundant phylum [24]. Moreover, several studies have demonstrated that endophytic *Streptomyces* are capable of producing bioactive compounds [25-27].

However, antimicrobial resistance (AMR) remains a major clinical challenge. Gram-negative bacterial strains (GNB) such as *Klebsiella*, *Escherichia* and Gram-positive *e.g. Staphylococcus* are the most dangerous pathogens in healthcare associated infections. As a result of such infections, the most commonly used antibiotics are no longer effective, a problem made worse by the emergence of antibiotic-resistant bacteria. It is, therefore, imperative to prevent and combat AMR infections in order to decrease the mortality rate of patients. In recent years, there has been a dramatic interest in discovering natural drugs, but the focus should be on identifying novel strains from unexplored habitats to discover new antibiotics [28]. One underexplored source is endophytic *Streptomyces* from medicinal plants for natural compounds. In line with our ongoing research on isolating potential endophytes with novel sources of natural compounds, we isolated *Streptomyces* sp. CR 13 from the roots of *Ocimum tenuiflorum* L. to assess antibacterial drug leads. Furthermore, *Streptomyces* sp. CR 13 was polytaxonamically characterized and its potential to synthesize silver nanoparticles (AgNPs) extracellularly was evaluated for its antibacterial properties.

EXPERIMENTAL

The chemicals and reagents used in this study were obtained from Sigma-Aldrich (Merck, India) and Himedia (Mumbai, India) and used without further purification.

Isolation & characterization of endophytic *Streptomyces* sp.

Plant material: Healthy *Ocimum tenuiflorum* L. plants were collected in sterile polythene bags from the foothills of Yercaud city (latitude: 11º20′-44º62′ N, longitude: 78º-35º57′31 E), India and stored in iceboxes at 4 ºC. The plant samples were analyzed within 12 h of collection.

Surface sterilization of plant: All the soil particles were removed from the root segments by running tap water. The plant tissue samples were then dried in a laminar air flow chamber. Roots were then chopped into the small pieces before surface sterilization. A previously described method was used for surface sterilization [29]. After that the tissue samples were rinsed in 0.1% Tween 20 for 30 s. The tissues were then immersed for 5 min in 70% ethanol (v/v) followed by immersion in 2% sodium hypochlorite solution for 10 min in order to inhibit the fungal growth. After that the tissues were rinsed three times with sterile water. In a laminar airflow chamber, the tissues were then thoroughly dried. Root tissues were then aseptically dissected and plated onto antibiotic-supplemented selective media (starch casein agar).

Isolation of endophytic *Streptomyces* and preservation: In this study, endophytic *Streptomyces* were isolated in the same manner as described by Verma *et al.* [29] with some modifications. Surface sterilized root segments were placed on starch casein agar medium containing (25 µg/mL), nystatin (25 µg/mL) and nalidixic acid (20 µg/mL) to inhibit the fungal and non-filamentous bacterial growth. Plates were incubated at 28 ºC for 3 weeks. Colonies of *Streptomyces* were observed to have a tough leathery texture, be dry or folded, to have branching filaments with or without aerial mycelia and to have spores. The pure cultures were obtained by streaking them repeatedly on ISP2 media (HI MEDIA Labs, India). Surface sterilization was validated as previously described [30]. The isolated pure cultures were stored in 25 % (v/v) glycerol solution at -20 ºC for further experimentations.

Characterization of endophytic *Streptomyces*: The morphological characterization was done according to the method as described by Shirling & Gottlieb [31]. Visual observation of general morphology was performed by light microscope. The ornamentation of the spore surface was analyzed by scanning electron microscopy (SEM model, JEOL-JSM 6390, Japan). Utilization of carbon and nitrogen sources was determined according to Miller [32]. Colonial features of aerial spore mass colour, substrate mycelial pigmentation and the colour of diffusible pigments were recorded on different media including ISP2, ISP3, ISP4, ISP5, ISP6 and ISP7. All plates were incubated at 28 ºC for 14 days. *Streptomyces* sp. CR13 was tested on ISP2 medium for pH, temperature and salinity tolerance. To test the effect of pH, the medium was adjusted to pH (5.0, 7.0, 9.0 and 11) and saline concentration (0, 2, 4, 6, 8 and 10% NaCl) and incubated at 28 ºC for 7 days. The strain was incubated at different temperatures (4, 28, 37, 45 and 50 ºC) for 7 days to determine the temperature effect. Determination of the cell wall isomer diaminopimelic acid (A2pm) was carried out using thin layer chromatography [33]. Genomic DNA of the strain was isolated according to the method as described by Hopwood *et al.* [34]. The quality and quantity of genomic DNA of the isolate were measured by a Nanodrop ND-2000 UV-visible spectrophotometer. The 16S rRNA gene of isolate was amplified by PCR using a pair of universal 27f 5'-AGAGTTTGATCMTGGCTCAG-3' and 1492 r 5'-GGTTACCTTGTTACGACTT-3' primers.

The PCR amplifications were conducted on a thermal cycler (Eppendorf, Germany). The PCR was performed in a final volume of 30 µL containing 0.5 µM of each primer, 1 µL of extracted DNA (50 ng), 5 µL of sterile distilled H_2O and 10% (v/v) of DMSO to the final volume in PCR premix (Emerald, Takara, Japan). Additionally, a negative control reaction mixture was prepared without the isolate's DNA template. PCR conditions were as follows: 5 min at 95 °C followed by 35 cycles of 1 min at 94 ºC, 1 min at 58 ºC and 3 min at 72 ºC followed by 10 min final extension at 72 ºC. PCR products were purified from 1% agarose gel (w/v) and sequenced on an ABI 310 automatic DNA sequencer (Applied Biosystems). BioEdit software and BLAST network services at the NCBI were used to analyze the resulting 16S rRNA gene sequence [35,36]. Multiple alignments were performed using the CLUSTAL_X version 1.8 [37]. Phylogenetic tree was inferred neighbor-joining method with MEGA 11 software package [38,39]. The unrooted phylogenetic tree topology was evaluated by using the bootstrap resampling method with 1000 replicates [40].

Preparation of cell free extract from *Streptomyces* sp. CR13: *Streptomyces* sp. CR13 was cultured for 5 days at 28 ºC and 220 rpm in ISP2 medium. For the preparation of cell-free extract, the culture broth was centrifuged at 8000x g for 5 min at 4 ºC and then filtered through polyethersulfone (PES) high flow syringe filters (Sartorius Minisart® high flow Syringe

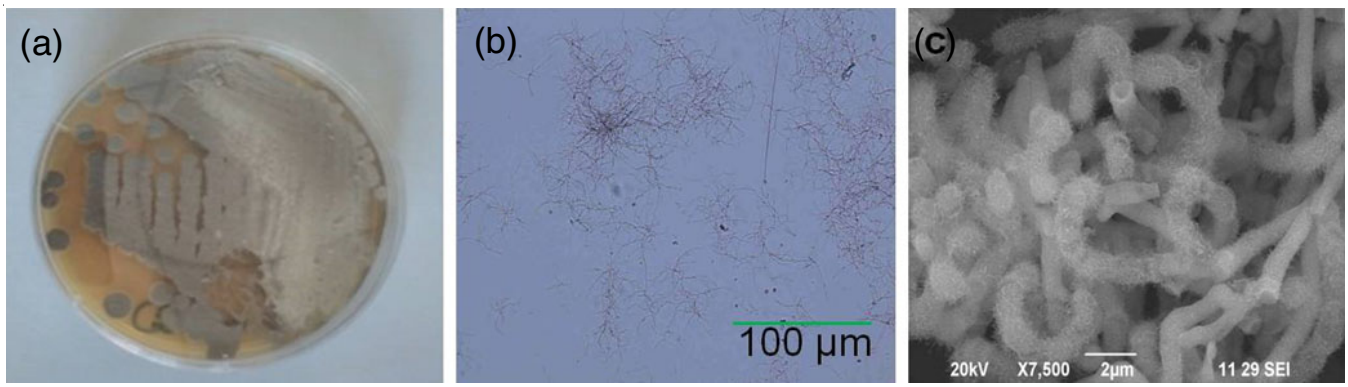

Fig. 1. (a) *Streptomyces* sp. CR 13; (b) morphology of filamentous *Streptomyces* sp. CR 13 in shake flask cultures; (c) scanning electron micrograph of the spore morphology of endophytic *Streptomyces* sp.CR13 grown on ISP2 media at 28 °C for 14 days

Filters). The supernatants were then used for synthesizing silver nanoparticles.

Fabrication of endophytic *Streptomyces* sp. CR13 derived StrAgNPs: An aqueous filtrate of *Streptomyces* sp. CR13 was used as a reducing agent in an aqueous $AgNO_3$ solution to fabricate StrAgNPs. In order to synthesize StrAgNPs, 10 mL of filtrate was mixed with 90 mL of 1 mM $AgNO_3$ solution. It was then incubated at room temperature for 1 to 3 days under dark conditions.

Characterization of StrAgNPs: The colour formation of the reaction changed after incubation, indicating the presence of StrAgNPs. StrAgNPs were measured between 300 and 700 nm using UV-visible spectrophotometer for surface plasmon resonance (SPR). In the cell-free extract, the functional groups could reduce, cap and stabilize StrAgNPs. Fourier transform infrared spectroscopy analysis was performed using a JASCO Fourier transform infrared spectrometer in the range of 4000-400 cm^{-1} to determine the functional groups. The X-ray powder diffractometer (XPD) analysis was conducted on StrAgNPs to explore their crystallographic structure and orientation (λ = 0.1546 nm) (Rigaku Ltd., Tokyo, Japan). Transmission electron microscopy (TEM) exclusively characterized the morphological features (size and shape) of StrAgNPs using a JEOL 3010 transmission electron microscope. A Zetasizer Nano (ZS 90) was used to measure the zeta potential of synthesized StrAgNPs. The synthesized StrAgNPs were sonicated for 10-20 min to disperse the nanoparticles and analyzed with the Malvern Zetasizer Nano-ZS90.

Antibacterial activity: Two Gram-negative strains *K. pneumonia* (MTCC-4030), *E. coli* (MTCC-433) and one Gram-positive (S. *aureus* MTCC690) was tested in this study. The bacterial cultures were inoculated with Mueller- Hinton and grown overnight at 37 ºC. By using a cotton swab, bacteria cultures with about 10^6 CFU/mL were spread evenly over the Mueller-Hinton plate. A diameter of 6 mm wells were prepared with a sterile cork borer. Wells were then loaded with different volumes of StrAgNPs (10, 30, 50 and 60 µL) and incubated at 37 ºC for 24 h. With control of cell-free extract, the assay was performed in triplicate. A 50 µL of DMSO was used as a negative control adnd the ZOIs were measured in diameter (mm).

Statistical analysis: SPSS 16.0 edition was used for the statistical analysis (SPSS Inc., Chicago, IL, USA). An ANOVA (post-hoc Tukey's test) was used in antibacterial studies to determine the statistical differences.

RESULTS AND DISCUSSION

The *Streptomyces* sp. CR13 strain was isolated from root tissues of *Ocimum tenuiflorum* L. A typical filamentous growth with good spore formation was observed after 3 weeks of incubation at 28 ºC on starch casein agar medium. Surface sterilized solution did not produce microbial growth on starch casein agar media indicating that the isolated strain is endophytic. Further, no growth was observed when the colony was treated with sterilizing solutions. As shown in Fig. 1a, after 7 days of growth on ISP2, the isolate has developed gray to white coloured spores. Light microscopic analysis revealed a distinct well branched aerial and substrate mycelium (Fig. 1b). The SEM analysis showed that spore chains had single branched and long aerial mycelia with smooth surfaces (Fig. 1c). For morphological and cultural characteristics, the isolate was grown on ISP2, ISP3, ISP4, ISP5, ISP6 and ISP7. Strain morphological and structural characteristics are presented in Table-1. This isolate had L,L-2,6-diaminopimelic acid (Fig. 2) in its cell wall peptidoglycan, characteristic of *Streptomyces*. Based on the isolate's 16S rRNA gene sequence (1458 nt), strain CR 13 belongs to the genus *Streptomyces* (Fig. 3). Based on the results of morphological, physiological, chemotaxonomic and genomic analyses, the strain was named *Streptomyces* sp. CR 13.

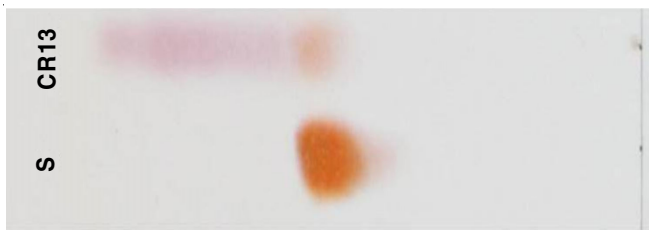

Fig. 2. Thin layer chromatography of cell wall isomer diaminopimelic acid (A2pm); S: standard (2,6-diaminopimelic acid (0.01 M); CR13: isomer A2pm extracted from *Streptomyces* sp. CR 13 cell wall

Characterization of StrAgNPs: The cell-free extract containing secondary metabolites of *Streptomyces* sp. CR 13 was incubated at 30 ºC with an equal volume of 1 mM $AgNO_3$ solution. Within 24 h incubation, it was observed that the reaction

TABLE-1
PHENOTYPIC, BIOCHEMICAL AND CULTURAL CHARACTERISTICS OF *Streptomyces* sp. CR13

Characteristics	*Streptomyces* sp. CR13					
Features	ISP2	ISP3	ISP4	ISP5	ISP6	ISP7
Growth	Good	Good	Good	Moderate	Poor	Moderate
Sporulation	Good	Good	Good	Moderate	Poor	Moderate
Colour of substrate mycelium	Gray	Light Gray	Light black	Light white	White	Blackish gray
Colour of the aerial mycelium	Whitish gray	Gray	Gray	Dark gray	White	Gray
Diffusible pigment	Light black	–	–	–	–	–

Biochemical		Utilization of carbon		Growth on sole nitrogen source	
Gram staining	Positive	L-Arabinose	+++	Alanine	–
Citrate utilization	Negative	Dextrose	+++	Arginine	++
Methyl Red	Negative	Fructose	+++	Asparagine	–
Voges-Proskauer	Negative	Inosittol	++	Cysteine	–
H2S production	Negative	Lactose	–	Methionine	–
Nitrate reduction test	Positive	Mannitol	++	Phenylalanine	–
Catalase test	Negative	Maltose	++		
Urea hydrolysis	Negative	Sucrose	+++		
Gelatin hydrolysis	Negative	Raffinose	++		
Starch hydrolysis	Positive	Xylose	++		

Effect of temperature on growth	4 °C	28 °C	37 °C	40 °C	45 °C	50 °C
	–	+++	+++	+	–	–
Effect of pH on growth	pH 5	pH 7	pH 9	pH 11		
	+	+++	+++	–		
Effect of NaCl (%) concentration on growth	0%	2%	4%	6%	8%	10%
	+++	+++	+++	+++	–	–

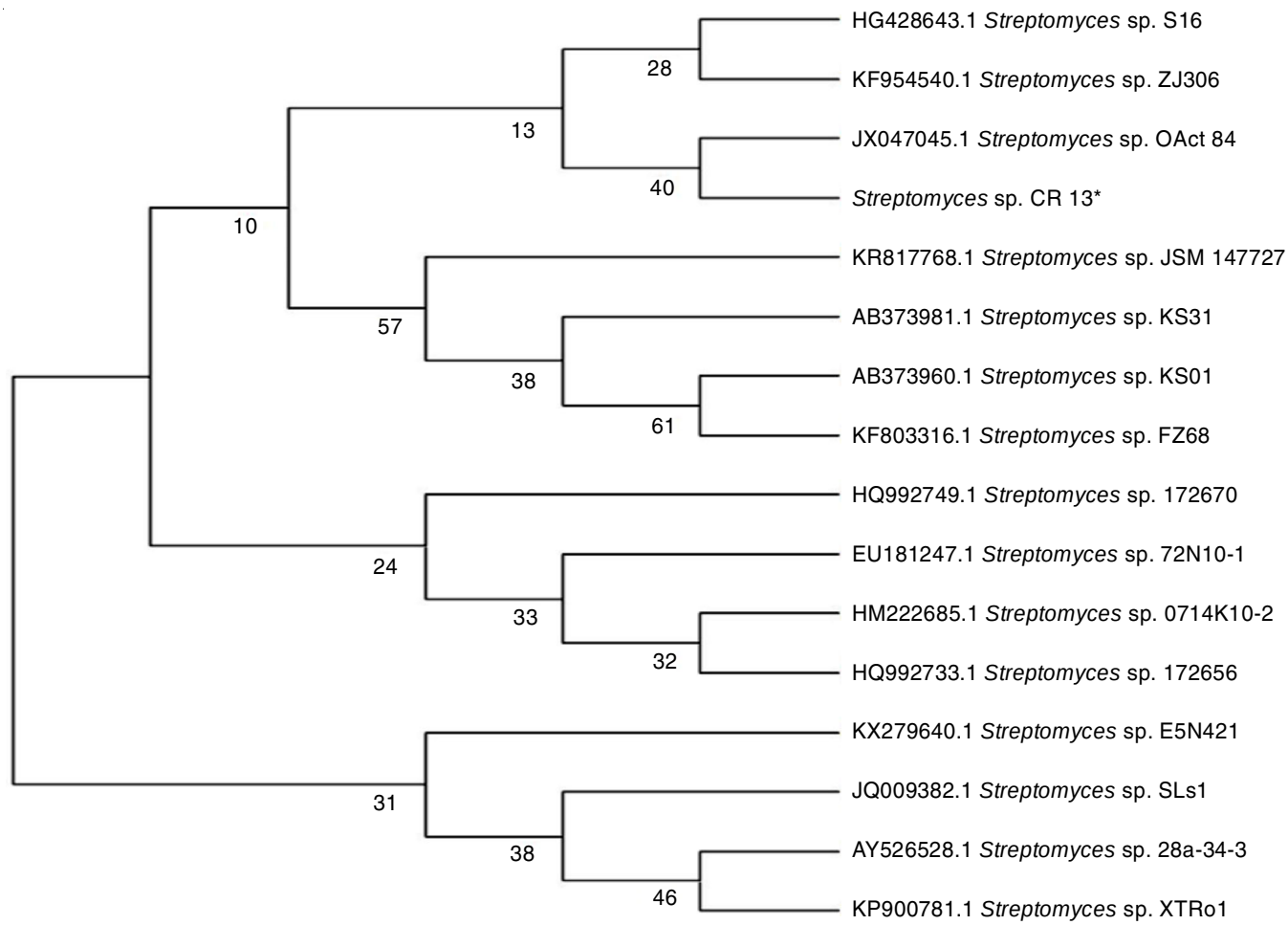

Fig. 3. Phylogenetic tree of *Streptomyces* sp. CR 13 was inferred using the neighbour-joining method using MEGA 11 program. The Bootstrap values above 50%, presented as percentages of 1000 replications, are shown at the branch points

mixture's colour had changed from pale yellow to a dark brown, which is a clear indication that biogenic AgNPs had formed (Fig. 4). Control reaction mixture ($AgNO_3$) without cell free extract mixture showed no colour change (Fig. 4). With increasing incubation time, the colour intensity has been increased. This brown colour is due to surface plasmon resonance (SPR), a characteristic of biosynthesized nanoparticles [41]. The present results are in agreement with those in previous studies, which found that SPR was responsible for colour change [42].

Different pH and cell-free extract concentrations affected the synthesis of AgNPs. According to colour change and UV-visible spectra at 425 nm peak absorbance, the optimal extract concentration is 1:9 (Fig. 5a). To maximize the synthesis of

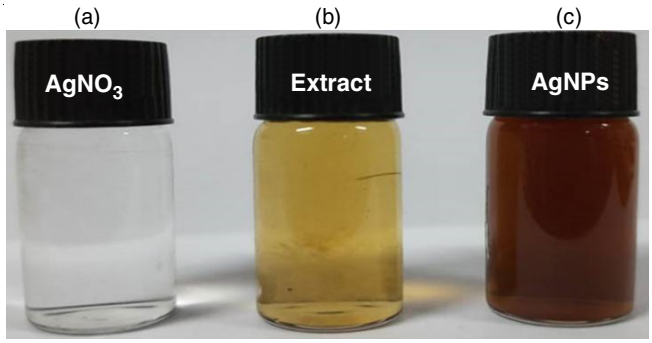

Fig. 4. Colour change profile of biosynthesized AgNPs, (a) $AgNO_3$: silver nitrate solution; (b) cell free extract; (c) biosynthesized AgNPs ($AgNO_3$ + cell free extract)

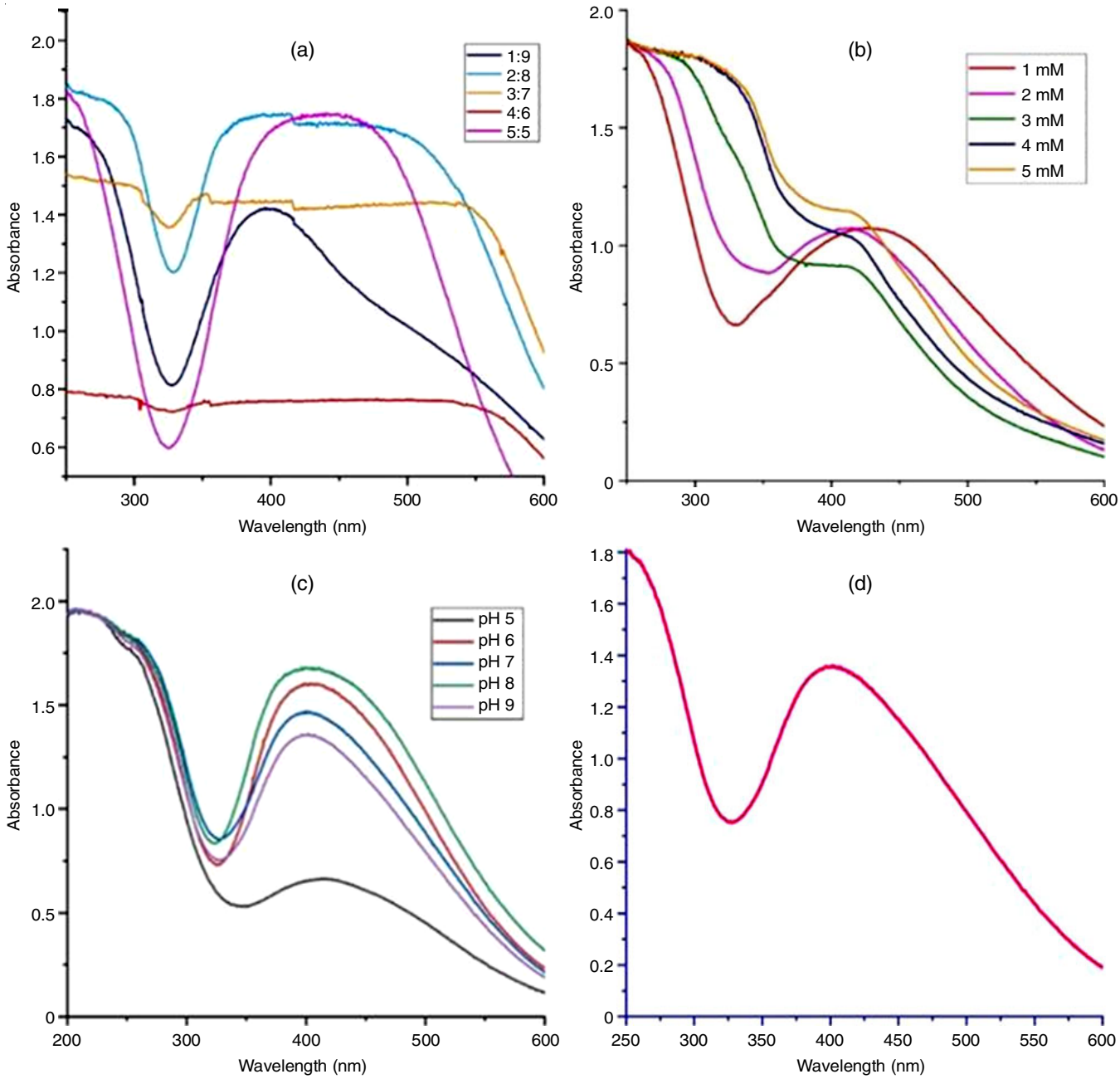

Fig. 5. Colour change formation and optimization of StrAgNPs, (a) UV absorption spectrum of StrAgNPs (culture extract *vs.* silver nitrate), (b) effect of pH on the synthesis of StrAgNPs, (c) effect of temperature on the synthesis of StrAgNPs, (d) UV-visible spectroscopy produced intense SPR spectra at 425 nm in optimized conditions

AgNPs, the effects of different concentrations of $AgNO_3$ from 1 mM to 5 mM were also investigated. Blending cell-free extract with 1 mM, $AgNO_3$ exhibited a significant increase in absorption with a peak centered at 425 nm (Fig. 5b). At pH 9.0, the strong peak occurs at 425 nm, which indicates the presence of uniform-size nanoparticles (Fig. 5c). Conversely, a decrease in pH to 5.0 did not show a peak. The aggregation of nanoparticles occurs at low pH because the protein structure is affected, resulting in the proteins being denatured and losing their activity. The stability of capping proteins suggests that proteins present in the reaction mixture for the capping of AgNPs are stable at pH 9.0. The results of this study were in agreement with those reported by Singh *et al.* [43].

The FT-IR analysis was used to identify different functional groups involved in the reduction of Ag^+ ions and capping of StrAgNPs. The FT-IR spectra (Fig. 6) show the prominent peaks at 3373, 2831, 1654, 1401 and 1015 cm^{-1}. The peak at 3373 cm^{-1} could be assigned to the O–H and N–H amine, while the peak at 2831 cm^{-1} represented the C–H stretching of the protein's functional groups in the cell-free extract. It was also observed that at 1654 cm^{-1} may be attributed to the –CO of the amide-I band of the proteins; the peak at 1407 cm^{-1} was due to the C–N stretching vibrations of the aromatic amines. Thus, proteins in the cell free extract may have acted as reducing and stabilizing agents for biogenic StrAgNPs, according to the FT-IR analysis.

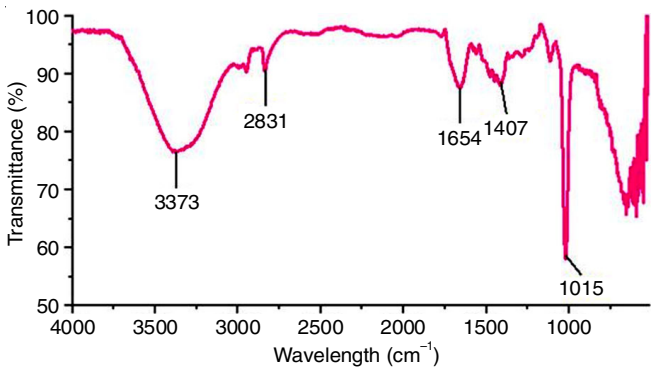

Fig. 6. FT-IR analysis of biogenic AgNPs

The XRD analysis was used to determine the crystalline nature of AgNPs. The well-defined diffraction peaks (Fig. 7) were observed in the spectra at 2θ values of 38.2º, 44.4º, 64.3º, 77.5º attributed to (111), (200), (220), (311), respectively (JCPDS No. 03-0921). Silver nanocrystals were well described by the obtained peaks, which were in good agreement with unit cells found in face-centered cubic structures. Additionally, an unassigned peak at 28.05º could represent the crystallization of proteins or secondary metabolites.

The DLS results showed that the particles had a size of 30.40 nm (Fig. 8a). An analysis of the zeta potential of StrAgNPs revealed that the particles were highly stable, with a charge of -35.2 mV (Fig. 8b). It is evident that biosynthesized silver nanoparticles are not aggregated in aqueous solutions. The morphology and shape of StrAgNPs were determined using TEM measurements. The TEM micrograph (Fig. 8c) reveals that

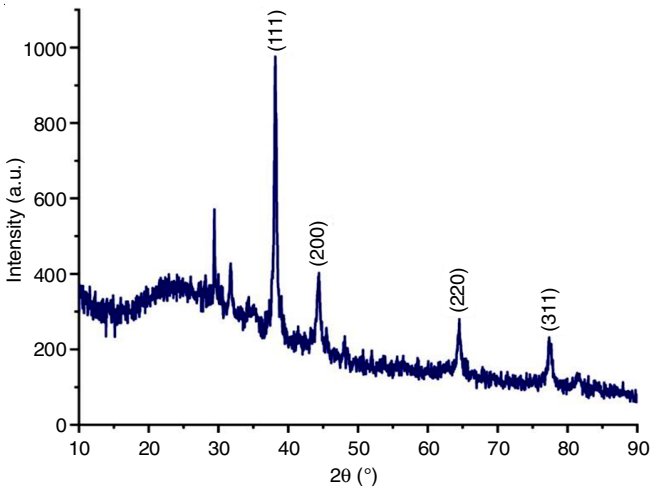

Fig. 7. X-ray diffraction pattern of biosynthesized AgNPs

the particle is small, spherical and well dispersed without agglomeration. The AgNPs were spherical in shape with sizes between 18 nm and 21 nm, according to TEM analysis. This finding is consistent with previous studies showing StrAgNPs synthesized from cell free extract were spherical in shape [41,44]. The SAED patterns recorded for single particles in the aggregated nanoparticle samples corresponded to a typical polycrystalline ring pattern. This finding revealed that the nanoparticles synthesized were crystalline in nature.

Antibacterial activity: The bacterial inhibitory effects of biosynthesized AgNPs on *E. coli*, *K. pneumoniae* and *S. aureus* using well diffusion method was conducted. Compared to cell-free extract alone, biosynthesized StrAgNPs showed more potent antibacterial activity (Fig. 9). The highest zones of inhibition (ZOI) were 18 ± 0.3 mm, 16 ± 0.8 mm and 15 ± 0.3 mm for *E. coli*, *K. pneumoniae* and *S. aureus* at 60 µL, respectively. As a result of their non-toxic effects on human cells at low concentrations and the fact that bacteria are less likely to develop resistance to silver ions, AgNPs have gained interest as a promising antimicrobial agent [45]. Several studies have postulated mechanisms associated with AgNPs' bactericidal properties. When AgNPs are close to bacteria or their surroundings, their high surface/mass ratio of Ag^+ can result in higher microbicidal effects [46]. A size-dependent interaction of AgNPs with bacteria has also been reported [47].

Conclusion

In this work, an endophytic *Streptomyces* sp. CR13 cell-free extract was used to synthesize silver nanoparticles and characterized. It was found that the biosynthesized AgNPs had an ideal surface plasmon resonance (SPR) at 425 nm and a size range ranging from 18 to 21 nm. The pH value of 9 and the $AgNO_3$ concentration of 1 mM were optimal for synthesizing small nanoparticles from cell-free extracts. The FTIR analysis revealed proteins and other secondary metabolites acting as capping and reducing agents. The biogenic AgNPs displayed significant antibacterial activity against *E. coli*, *K. pneumoniae* and *S. aureus*. As a result, AgNPs can be synthesized at low costs in large quantities, which could lead to possible new applications in the antibacterial applications.

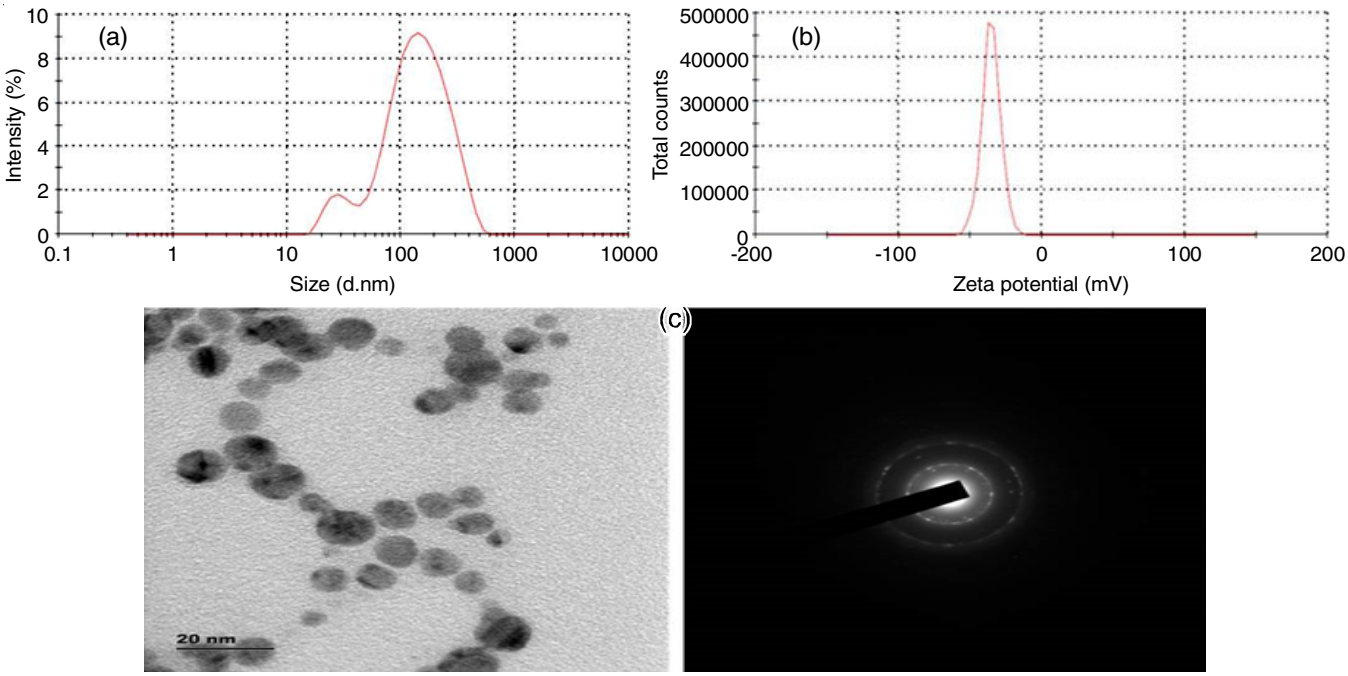

Fig. 8. (a) DLS analysis of StrAgNPs; (b) zeta potential of StrAgNPs; (c) TEM images for StrAgNPs and SEAD pattern

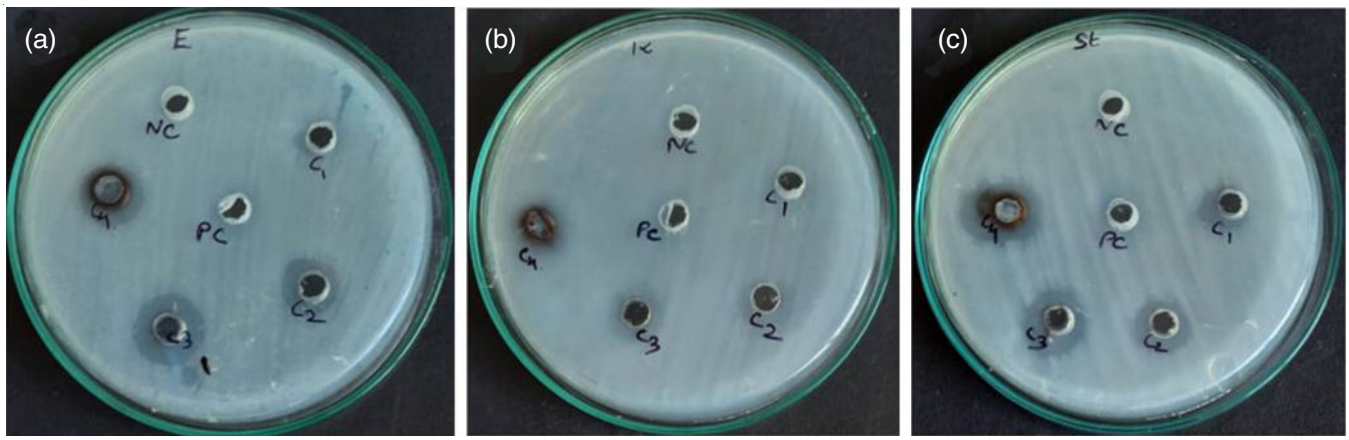

Fig. 9. Antibacterial activity of biosynthesized AgNPs, (a) *Escherichia coli*; (b) *Klebsiella pneumonia* and (c) *Stphylococcus aureus*

CONFLICT OF INTEREST

The authors declare that there is no conflict of interests regarding the publication of this article.

REFERENCES

1. I.X. Yin, J. Zhang, I.S. Zhao, M.L. Mei, Q. Li and C.H. Chu, *Int. J. Nanomedicine*, **15**, 2555 (2020); https://doi.org/10.2147/IJN.S246764
2. S. Iravani, H. Korbekandi, S.V. Mirmohammadi and B. Zolfaghari, *Res. Pharm. Sci.*, **9**, 385 (2014).
3. U. Rasool and S. Hemalatha, *Mater. Lett.*, **194**, 176 (2017); https://doi.org/10.1016/j.matlet.2017.02.055
4. C. Fang and M. Zhang, *J. Mater. Chem.*, **19**, 6258 (2009); https://doi.org/10.1039/b902182e
5. J. Boken, S.K. Soni and D. Kumar, *Crit. Rev. Anal. Chem.*, **46**, 538 (2016); https://doi.org/10.1080/10408347.2016.1169912
6. B. Zhang, R. Liang, M. Zheng, L. Cai and X. Fan, *Int. J. Mol. Sci.*, **20**, 3642 (2019); https://doi.org/10.3390/ijms20153642
7. H. Tian, J. Chen and X. Chen, *Small*, **9**, 2034 (2013); https://doi.org/10.1002/smll.201202485
8. H. Matusiewicz, *Acta Biomater.*, **10**, 2379 (2014); https://doi.org/10.1016/j.actbio.2014.02.027
9. E.M.A. Jamal, D.S. Kumar and M.R. Anantharaman, *Bull. Mater. Sci.*, **34**, 251 (2011); https://doi.org/10.1007/s12034-011-0071-y
10. Y. Benrighi, N. Nasrallah, T. Chaabane, V. Sivasankar, A. Darchen and O. Baaloudj, *Opt. Mater.*, **115**, 111035 (2021); https://doi.org/10.1016/j.optmat.2021.111035
11. L. Wang, Y. Wu, J. Xie, S. Wu and Z. Wu, *Mater. Sci. Eng. C*, **86**, 1 (2018); https://doi.org/10.1016/j.msec.2018.01.003
12. F. Martinez-Gutierrez, L. Boegli, A. Agostinho, E.M. Sánchez, H. Bach, F. Ruiz and G. James, *Biofouling*, **29**, 651 (2013); https://doi.org/10.1080/08927014.2013.794225
13. S. Parveen, A.H. Wani, M.A. Shah, H.S. Devi, M.Y. Bhat and J.A. Koka, *Microb. Pathog.*, **115**, 287 (2018); https://doi.org/10.1016/j.micpath.2017.12.068
14. C. Li, J. Zhang, Y.J. Zu, S.F. Nie, J. Cao, Q. Wang, S.P. Nie, Z.Y. Deng, M.Y. Xie and S. Wang, *Chin. J. Nat. Med.*, **13**, 641 (2015); https://doi.org/10.1016/S1875-5364(15)30061-3

15. N. Jain, P. Jain, D. Rajput and U.K. Patil, *Micro Nano Systems Lett.*, **9**, 5 (2021); https://doi.org/10.1186/s40486-021-00131-6
16. K.B. Narayanan and N. Sakthivel, *Adv. Colloid Interface Sci.*, **156**, 1 (2010); https://doi.org/10.1016/j.cis.2010.02.001
17. M. Moradi, Y. Vasseghian, A. Khataee, M. Harati and H. Arfaeinia, *Sep. Purif. Technol.*, **261**, 118274 (2021); https://doi.org/10.1016/j.seppur.2020.118274
18. G.H. Kelemen and M.J. Buttner, *Curr. Opin. Microbiol.*, **1**, 656 (1998); https://doi.org/10.1016/S1369-5274(98)80111-2
19. J. Bérdy, *J. Antibiot.*, **58**, 1 (2005); https://doi.org/10.1038/ja.2005.1
20. P. S.S, H.A. Rudayni, A. Bepari, S.K. Niazi and S. Nayaka, *Saudi J. Biol. Sci.*, **29**, 228 (2022); https://doi.org/10.1016/j.sjbs.2021.08.084
21. S. Hasegawa, A. Meguro, M. Shimizu, T. Nishimura and H. Kunoh, *Actinomycetologica*, **20**, 72 (2006); https://doi.org/10.3209/saj.20.72
22. A. Matsumoto and Y. Takahashi, *J. Antibiot.*, **70**, 514 (2017); https://doi.org/10.1038/ja.2017.20
23. M. Marian, T. Ohno, H. Suzuki, H. Kitamura, K. Kuroda and M. Shimizu, *Microbiol. Res.*, **234**, 126428 (2020); https://doi.org/10.1016/j.micres.2020.126428)
24. D.B. Müller, C. Vogel, Y. Bai and J.A. Vorholt, *Annu. Rev. Genet.*, **50**, 211 (2016); https://doi.org/10.1146/annurev-genet-120215-034952
25. P.T. Hong-Thao, N.V. Mai-Linh, N.T. Hong-Lien and N.V. Hieu, *Int. J. Microbiol.*, **2016**, 7207818 (2016); https://doi.org/10.1155/2016/7207818
26. K. Supong, C. Thawai, W. Choowong, C. Kittiwongwattana, P. Koohakan, D. Thanaboripat, C. Laosinwattana, N. Parinthawong and P. Pittayakhajonwut, *Res. Microbiol.*, **167**, 290 (2016); https://doi.org/10.1016/j.resmic.2016.01.004
27. T. Liu, Z. Ren, W.X. Chunyu, G.D. Li, X. Chen, Z.T. Zhang, H.B. Sun, M. Wang, T.P. Xie, M. Wang, J.Y. Chen, H. Zhou, Z.T. Ding and M. Yin, *Front. Microbiol.*, **13**, 831174 (2022); https://doi.org/10.3389/fmicb.2022.831174
28. M. Kamjam, P. Sivalingam, Z. Deng and K. Hong, *Front. Microbiol.*, **8**, 760 (2017); https://doi.org/10.3389/fmicb.2017.00760
29. V.C. Verma, S.K. Gond, A. Kumar, A. Mishra, R.N. Kharwar and A.C. Gange, *Microb. Ecol.*, **57**, 749 (2009); https://doi.org/10.1007/s00248-008-9450-3
30. Y. Goudjal, O. Toumatia, N. Sabaou, M. Barakate, F. Mathieu and A. Zitouni, *World J. Microbiol. Biotechnol*., **29**, 1821 (2013); https://doi.org/10.1007/s11274-013-1344-y
31. E.B. Shirling and D. Gottlieb, *Int. J. Syst. Evol. Microbiol.*, **16**, 313 (1966).
32. J.H. Miller, A Short Course in Bacterial Genetics A Laboratory Manual and Handbook for Escherichia coli and Related Bacteria, Cold Spring Harbor Laboratory Press, Cold Spring Harbor (1992).
33. T. Hasegawa, M. Takizawa and S. Tanida, *J. Gen. Appl. Microbiol.*, **29**, 319 (1983); https://doi.org/10.2323/jgam.29.319
34. D.A. Hopwood, M.J. Bibb and K.F. Chater, *Biochem. Educ.*, **14**, 196 (1986).
35. S.F. Altschul, T.L. Madden, A.A. Schäffer, J. Zhang, Z. Zhang, W. Miller and D.J. Lipman, *Nucleic Acids Res.*, **25**, 3389 (1997); https://doi.org/10.1093/nar/25.17.3389
36. T.A. Hall, BioEdit: A User-friendly Biological Sequence Alignment Editor and Analysis Program for Windows 95/98/NT, in: Nucleic acids Symposium Series, [London]: Information Retrieval Ltd., c1979-c2000, pp. 95-98 (1999).
37. J.D. Thompson, T.J. Gibson, F. Plewniak, F. Jeanmougin and D.G. Higgins, *Nucleic Acids Res.*, **25**, 4876 (1997); https://doi.org/10.1093/nar/25.24.4876
38. N. Saitou and M. Nei, *Mol. Biol. Evol.*, **4**, 406 (1987); https://doi.org/10.1093/oxfordjournals.molbev.a040454
39. K. Tamura, G. Stecher, D. Peterson, A. Filipski and S. Kumar, *Mol. Biol. Evol.*, **30**, 2725 (2013); https://doi.org/10.1093/molbev/mst197
40. J. Felsenstein, *Evolution*, **39**, 783 (1985); https://doi.org/10.2307/2408678
41. S. Sadhasivam, P. Shanmugam and K. Yun, *Colloids Surf. B Biointerfaces*, **81**, 358 (2010); https://doi.org/10.1016/j.colsurfb.2010.07.036
42. P. Manivasagan, K.H. Kang, D.G. Kim and S.K. Kim, *Int. J. Biol. Macromol.*, **77**, 159 (2015); https://doi.org/10.1016/j.ijbiomac.2015.03.022
43. B.A. Chopade, R. Singh, P. Wagh, S. Wadhwani, S. Gaidhani, A. Kumbhar and J. Bellare, *Int. J. Nanomedicine*, **8**, 4277 (2013); https://doi.org/10.2147/IJN.S48913
44. M. Manimaran and K. Kannabiran, *Lett. Appl. Microbiol.*, **64**, 401 (2017); https://doi.org/10.1111/lam.12730
45. K. Prabakar, P. Sivalingam, S.I. Mohamed Rabeek, M. Muthuselvam, N. Devarajan, A. Arjunan, R. Karthick, M.M. Suresh and J.P. Wembonyama, *Colloids Surf. B Biointerfaces*, **104**, 282 (2013); https://doi.org/10.1016/j.colsurfb.2012.11.041
46. D. Feng, R. Zhang, M. Zhang, A. Fang and F. Shi, *Nanomaterials*, **12**, 2636 (2022); https://doi.org/10.3390/nano12152636
47. A. Bakhtiari-Sardari, M. Mashreghi, H. Eshghi, F. Behnam-Rasouli, E. Lashani and B. Shahnavaz, *Biotechnol. Lett.*, **42**, 1985 (2020); https://doi.org/10.1007/s10529-020-02921-1